A REVIEW OF THE MAIMIK ROCKET EXPERIMENT

W. F. Denig
Geophysics Laboratory (AFSC)
Hanscom AFB, MA 01731-5000
and
B.N. Maehlum and K. Svenes
Norwegian Defense Research Institute (NDRE)
N-2007, Kjeller, NORWAY

ABSTRACT

The MAIMIK Mother-Daughter sounding rocket experiment has provided documented evidence of significant vehicle overcharging by an accelerator payload in the ionosphere. The instrumentation on the daughter included an electron gun system which injected 8-keV beams ranging from 20 mA to 800 mA into a low-density ionospheric plasma. The daughter and mother payloads were separated in-flight and electrically tethered during the early electron gun operations. The measured daughter potentials for the larger currents, at times, exceeded by 50% the nominal 8-keV beam energy. The effects of the beam-plasma interaction and the extreme vehicle charging were evident in the plasma and DC electric field instrumentation on the mother. The energy transfer from the beam to the ionospheric plasma, evidenced by an enhancement in the local electron temperature, maximized at 80 mA with no obvious indication of an anomalous ionization discharge mechanism. The transient electric fields measured at beam turn-on were consistent with the rapid charging of the daughter and the resulting ionospheric response. The three-fold purpose of the present report is to present an overview of the MAIMIK rocket experiment, review the evidence for the overcharging phenomenon, and discuss the relevent plasma and electric field observations.

INTRODUCTION

The MAIMIK experiment was a mother-daughter tethered sounding rocket originally conceived to address a number of crutial issues related to the electrodynamic behavior of an electron-emitting spacecraft in the ionosphere. The rationale for the experiment was based in part on the results of the earlier POLAR rocket series (Maehlum et al., 1980) as well as other investigations using artificial electron beams in space (Hess et al, 1971; Cambou et al., 1975; Winckler; 1980). These experiments had demonstrated the non-classical behavior of the interaction between the charged beam and the ionosphere which resulted in enhanced ionization production rates, extreme heating of the background plasma, and the generation of intense plasma waves. Although important contributions to the basic understanding of the beam-plasma interaction were made by a number of laboratory experiments (Bernstein et al., 1979; Grandal, 1982) the applicability of these studies to the space environment had not been well established (and still isn't). The specific issues proposed for further investigation by the MAIMIK rocket experiment were; 1) the energy transfer mechanism from the beam to the background plasma and its dependence on varying beam currents and changing atmospheric density, 2) measurement of the time constants for the relaxation of the ionosphere following the termination of the beam, 3) determination of the physical dimensions of the disturbed ionospheric region, and 4) an investigation of the charging processes for a beam-emitting spacecraft and a tethered companion payload.

The MAIMIK rocket experiment was conducted under the auspices of the Royal Norwegian Council for Scientific and Industrial Research (NTNF) and the National Aeronautics and Space Administration (NASA). Payload integration was conducted by the Norwegian Defense Research Establishment (NDRE) and launch activities coordinated at the Andoya Rocket

Range (69°17'39" N, 16°01'15"). The project scientist for the MAIMIK rocket experiment was Dr. B.N. Maehlum (NDRE) with participating scientists from Norway, the USA, Sweden, and Austria. Supporting ionospheric measurements at the time of the flight were made by the European Incoherent Scatter (EISCAT) radar facility.

The principal findings from the MAIMIK rocket experiment have been the observations of an overcharging condition by the beam-emitting payload, a current dependent peak in the beam to plasma energy transfer rate in the absence of an anomalous ionization source, and impulsive electric fields well outside of the heated plasma region which were driven by ion dynamics. This report is a summary of the important MAIMIK results which have been separately reported elsewhere (Maehlum et al., 1988; Svenes et al., 1988; Denig et al., 1989). However, we have also endeavored in the preparation of this report to combine these separate analyses by showing the interrelationships among the various topics.

INSTRUMENTATION

The MAIMIK sounding rocket was launched in a northwesterly direction into a quiet sub-auroral ionosphere at 18:56 UT on 10 November 1985. The payload section of the Terrier/Black Brant two-stage vehicle consisted of separate mother and daughter sections which were detached 62 s after launch with the aft-mounted mother remaining attached to the second stage motor. Following separation the velocity of the daughter relative to the mother payload remained a constant 0.8 m-s^{-1} at 23° to the local magnetic field. Attitude stability for both the mother and daughter payloads was maintained by their respective spin rates of 0.3 Hz and 3.3 Hz. The coning half-angle for the mother was 35° with a coning period of 300 s. The coning half-angle for the daughter was much less severe, being about 5°. The MAIMIK mother and daughter payloads reached an apogee of 381 km at 320 s.

During the interval between separation and 113 s, the mother and daughter payloads were electrically tethered through a 10 Megohm impedance. This time interval overlapped the initial electron gun operations which commenced at 101 s and continued throughout the remainder of the flight. The purpose of the tether was to provide a "mother" ground reference during

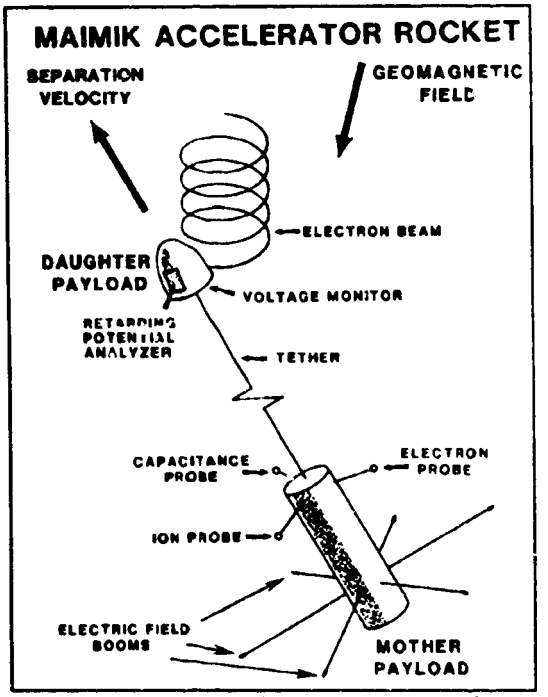

Figure 1. Schematic Illustration of the MAIMIK Rocket Experiment.

electron beam operations when the daughter was actively charged relative to the background plasma. The accuracy of the ground reference was futher maintained by keeping the conducting surface area of the mother (9.7 m^2) large compared to that of the active daughter (1.1 m^2). Although the mission plan was to keep the two payloads tethered until 130 s, the premature disconnection of the tether wire at 113 s limited the total amount of tether data available to 17 beam pulses over a full range of emission currents. The full complement of scientific instruments included in the MAIMIK rocket program is listed in Table 1. Unfortunately, the failure of a PCM encoder within the mother payload early in the flight had a catastrophic effect on the downlink data from the particle spectrometer, the VLF wave receivers, and the television camera. On the other hand, the analysis of the data from the HF

transmitter and receiver is presently ongoing but has little bearing on the present subject (K. Torkar, private communication, 1989). Figure 1 is a simplified schematic of the MAIMIK rocket payload detailing the instrument geometry for several of the experiments relevant to the present study. On the daughter payload the experiments included the electron accelerator, a set of electron retarding potential analyzers, and a tether voltage monitor. A daughter magnetometer was used to determine the beam injection pitch angle and to estimate the vehicle's instantaneous attitude. The mother instrumentation included a set of plasma probes and a three-axis electric field instrument. The MAIMIK mother attitude was determined by the NASA-Wallops Flight Facility (Reference: BBIX 36005) using the available gyro data and the higher time resolution data from an onboard magnetometer.

The electron accelerator system on the daughter payload consisted of a set of five identical gun units operated in an emission-limited diode configuration at a fixed accelerator voltage of 8 keV. Sequential 11-ms pulses of 320 mA, 80 mA, 40 mA, 20 mA, 40 mA, 80 mA, 160 mA, and 800 mA were injected into the ionosphere at a pulse repetition frequency of 1.2 Hz. For currents in the range 20 mA to 160 mA only a single gun head was used to generate the beam. However, the 320 mA and 800 mA current pulses required the simultaneous operation of two and five heads, respectively. The nearly DC beam operated at a high voltage chopper frequency of 1.2 kHz with a voltage ripple of less than 2 kV below the nominal accelerator voltage. The injection pitch angles ranged from 65° to 115° with an unfocused beam spread of less than 10°. Although the electron gun was instrumented to monitor the accelerator voltage and current, these data were carried on the telemetry channel that failed during the flight. The values used in the present analysis were from pre-flight calibrations.

Table I. Scientific Instrument Complement for the MAIMIK Rocket.

Daughter Payload
Electron Accelerator
Return Current Monitor
Voltage Monitor
Retarding Potential Monitor
HF Transmitter
Photometer Array
Mother Payload
DC E-field detector
TV Camera
Capacitance Probe
Ion Probe
Electron Temperature Probe
Fast Particle Spectrometer
VLF/HF Wave Receivers

The daughter's potential was measured using the tether voltage monitor (VM) and the electron retarding potential analyzers (RPA's). The tether connecting the mother and daughter payloads was an insulated stainless steel wire having a cross section of 0.2 mm^2. The differential voltage between the payloads was measured across a 10 Megohm resistor located in the active daughter payload. The VM output was linear between +10 V and -10 V and logarithmic between -10 V and -15 kV. Note that a negative VM signal indicated a positive daughter potential relative to the mother. The RPA consisted of an array of eight separate analyzer grids having fixed retarding potentials of 0 V, -12 V, -85 V, -180 V, -400 V, -800 V, -1.6 kV, and -3.2 kV relative to the daughter. The collecting area of each detector was 6.6 cm^2 and the minimum detectable current was 2 nA. The observed energy cut-off during positive charging of the daughter provided a redundant measure of the payload charging level. Although the RPA operated only over a limited energy range, the instrument did provide a continuous monitor of the daughter potential throughout the entire rocket flight well past tether disconnect at 113 s.

The set of mother plasma probes consisted of an electron temperature probe (ETP), an ion probe (IP), and a capacitance probe (CAP) each mounted on a separate 80-cm boom and deployed at 60 s. The ETP was a

Langmuir-type probe consisting of a spherical grid, 5 cm in diameter, surrounding a collector at a bias of +10V. The outer grid was swept both up and down between -1.9V and +4.9V relative to spacecraft ground with a "sweep" time of 13.1 ms. The general theory of gridded spherical sensors and their application for sounding rocket measurements has been discussed by Sagalyn et al. (1963). The IP was a 4-cm diameter solid spherical sensor held at a fixed bias voltage of -2V. The measurements included both the AC and DC components of the incoming ion flux. The CAP measured the capacitance of a 4.2 cm diameter floating probe immersed in the background plasma. During periods when the payload and plasma were not greatly disturbed the CAP was surrounded by a classic Debye sheath having a radial dimension proportional to the square root of the ratio of the electron density and temperature. The capacitance of this RF probe formed part of an LC-oscillator circuit which operated at a fixed frequency of 1 MHz (Balmain; 1966). Although the plasma probes had a nominal performance during the entire flight, prior to tether disconnect at 113 s the probe data was adversely affected by the mother charging during electron gun operations.

Vector electric fields at the location of the MAIMIK mother payload were measured using an orthogonal, three-axis set of double probes. Each double probe consisted of a cylindrical boom pair having 61 cm of bare wire at the extremes which contacted the plasma and whose potential was monitored through a 10^{12} ohm preamplifier impedance and referenced to the rocket body. The inner portion of each boom was insulated from the plasma by a coating of Kapton. As depicted in Figure 1, two of the boom pairs were mounted at 45° to the rocket spin axis while the third pair was in a plane perpendicular to the spin axis. The 45° booms were constructed of rigid stainless steel whose active elements had a nominal separation of 5.7 m. The third pair had a separation length of 8.8 m and were fabricated from a flexible Beryllium-Copper alloy. The electric field booms were deployed between 70 s and 100 s and were fully operational prior to the first gun pulse. Thereafter, the instrument had a nominal operation until re-entry. The components of the local electric field were derived in a straight-forward fashion as the negative of the potential difference between each boom pair divided by the boom length. The sensitivity of the vector instrument ranged from 3 $mV\text{-}m^{-1}$ (limited by the 8-bit telemetry system) to greater than 1 $V\text{-}m^{-1}$ at a maximum sampling frequency of 2.44 kHz. The measurements were corrected for motion-induced electric fields and for contact potential variations. During the main part of the flight the systematic errors associated with the data were determined to be no greater than 5 $mV\text{-}m^{-1}$. However, prior to 130 s major changes in the measured background field were caused by contact potential variations partially caused by outgassing of the rocket payload and energetic electron bombardment.

DATA

The MAIMIK launch criteria specified a darkened subauroral ionosphere and geomagnetic quiet conditions. The sounding rocket was launched in the absence of any visible auroral activity. Figure 2 is the background electron density and figure 3 is the ionospheric electric field measured by MAIMIK. The electron density profile for the ascent and descent phases of the flight was normalized to the EISCAT radar which measured an electron density of $4 \times 10^4\text{-}cm^{-3}$ and a temperature of 1500 °K near the

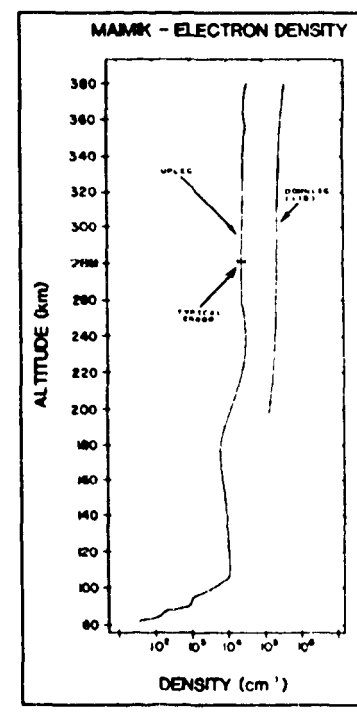

Figure 2. Measured electron densuty profile during rocket ascent and descent.

250-km F-region peak (T. Hanson, private communication, 1984). The MAIMIK measurements indicated that the density profile between 240 km and apogee was fairly constant with only a modest increase (50%) at the F-region peak. A 3-hour averaged K_p=3 level persisted for the 24 hours preceding the flight (Coffey, 1986) and overflights by the Defense Meteriological Satellite Program (DMSP) F7 satellite indicated that the Field-Aligned Currents (FAC) within the eveningside northern hemisphere were weak and consistent with a northward Interplanetary Magnetic Field (IMF). Although the main portion of the rocket flight was at subauroral latitudes it is likely that MAIMIK entered the auroral oval towards the end of the mission when

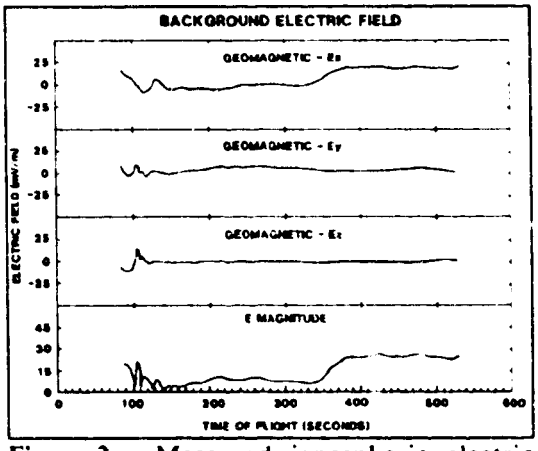

Figure 3. Measured ionospheric electric field for the MAIMIK flight.

the measured northward component of the ionospheric electric field sudden increased from near 0 to 26 mV-m^{-1} at 340 s. At the time of this transition, the rocket was situated at a geomagnetic latitude of 56° and at 19.6 MLT closely corresponding to the statistical location of the low-latitude auroral boundary for a K_p=3 (Hardy et al., 1985).

Figure 4 is a summary plot (lower curve) of the tether voltage monitor for the period between 100 s and 110 s which included the initial twelve electron beam pulses. The indicated 8-kV voltage level refers to the nominal energy of the beam electrons. Also shown in the top panel of figure 4 are the corresponding currents for each beam pulse. The sense of the tether voltage was the

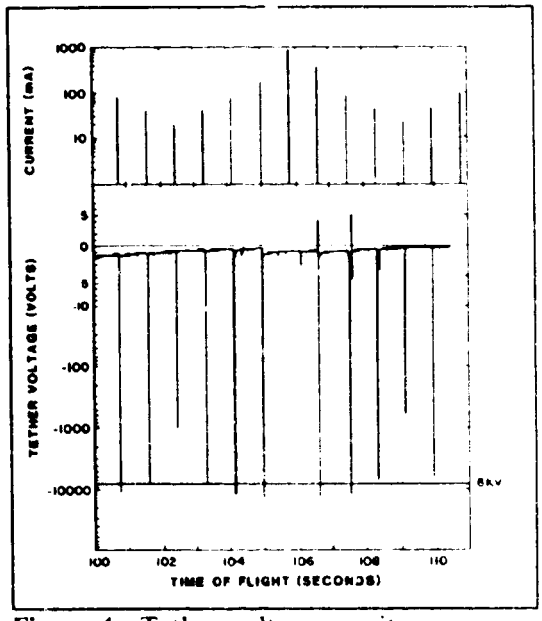

Figure 4. Tether voltage monitor.

potential of the "floating" daughter relative to the "grounded" mother where negative tether voltages indicated the positive charging of the active daughter payload. A comparison of the tether voltages with the daughter RPA confirm the proper operation of the tether system at least within the 0-to-3.2 keV energy range of the RPA (Maehlum et al., 1988). The tether measurements indicated that the daughter potential at times exceeded the energy of the beam by as much as 50% for beam currents greater than 40 mA. At 40 mA and below, the daughter charging was less than the beam energy although the charging level was still significant. Finally, we note that although the indicated 800-mA current pulse did occur, the tether voltage monitor data was lost due to an onboard telemetry system anomaly.

A more detailed look at the characteristics of the tether voltage during a sample 160-mA beam pulse is provided in figure 5. Note that the sudden change in the tether voltage corresponds to the start of the beam pulse and that high potentials were achieved within a telemetry sample period of beam turn-on. For the remainder of the beam the daughter potential oscillated at the 1.2 kHz frequency of the gun high voltage chopper

circuit. The maximum potential during the pulse reached about 14 kV or some 6 kV above the nominal beam energy. At beam termination, the daughter potential remained positive but dropped rapidly to within 10 eV of the mother and then decreased more gradually to zero over the next several milliseconds.

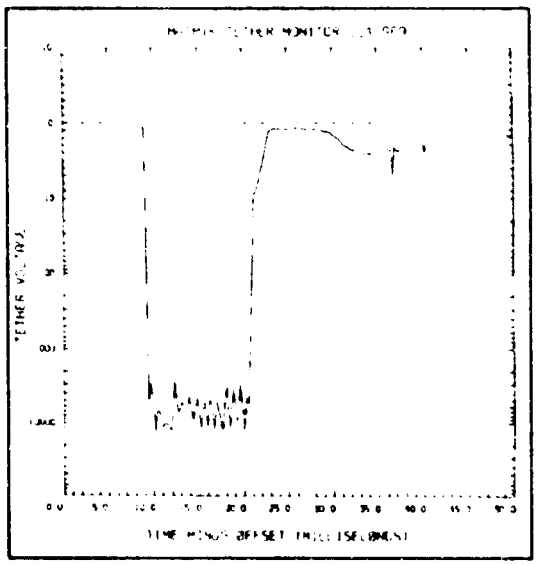

Figure 5. High time resolution VM measurements for a 160-mA beam.

The RPA measurements shown in figure 6 for the same 160 mA pulse sample confirm the rapid charging of the daughter payload at the initiation of the gun pulse and the persistent high charging level throughout the 11-ms pulse. The variations seen in some of the energy channels were perhaps associated with the oscillations in the daughter potential although the limited sampling frequency of the RPA channels does complicate the association. Following the termination of the beam and the rapid return towards zero of the daughter potential, the vehicle remained enveloped in a low density cloud of energetic electrons, up to 800 eV, which persisted for several tens of milliseconds. Although the daughter was moving out of the interaction region during these measurements the residual signal placed a lower limit on the relaxation

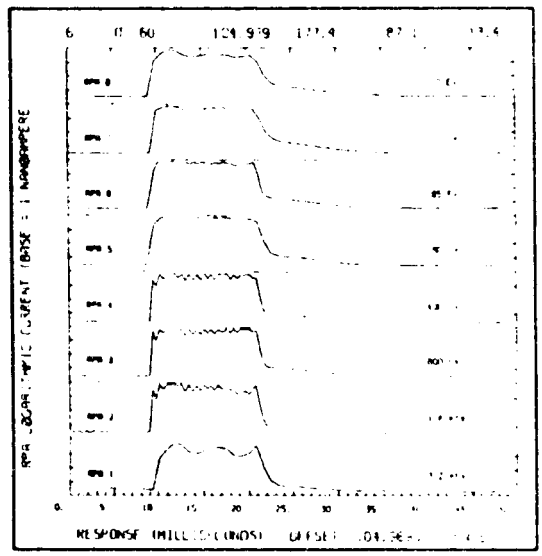

Figure 6. High time resolution RPA measurements for a 160 mA-beam.

time of the cloud.

The residual effects of the heated plasma region could also be seen in the tether monitor observations. The sample data in figure 5 indicates that the relative voltage between the mother and daughter had a broad but distinct peak centered several tens of milliseconds after the termination of the beam pulse. Note that there was no corresponding aftereffect in the RPA data of figure 6 suggesting that the signal was due to local effects near the mother. At the time of the broad voltage signature the mother was traversing the region of space formerly occupied by the beam-emitting daughter. The small negative charging of the vehicle must have been due to the mother moving into the residual hot plasma cloud.

The spatial and temporal characteristics of the heated plasma region were examined in more detail using the MAIMIK set of plasma probes on the mother payload (Svenes et al., 1988). The beam-induced effects were evident both during the injection pulses and as pulse aftereffects. There were also significant differences in the responses of the plasma probes relating to the tether and the analysis was therefore separated into observations made before and

after the tether disconnect.

Prior to the electrical separation at 114 s, the beam-induced responses in the plasma probes were adversely affected by the high charging of the daughter which tended to draw the mother payload somewhat positive. At the maximum charging level of 14 keV the tether current through the 10 Megohm impedance was 1.4 mA. On the other hand, the thermal flux at the mother for an ionospheric density and electron temperature of 4 x 10^4 cm^{-3} and 1500 °K, respectively, was 8.5 nA-cm^{-2} resulting in a total available thermal current of 0.8 mA to the mother payload (9.7 m^2 surface area). The slight charging of the mother payload was necessary to draw the additional current from the ionosphere.

The plasma probe pulse responses during the tether measurements were increases in the electron flux to the ETP and CAP probes and a decrease in the positive ion flux to the IP. Immediately after the termination of the beam pulse the potential of the mother decreased and the ETP returned to a more normal operation. ETP measurements made during the first Langmuir sweep after the beam showed enhanced electron temperatures well above background that were proportional to the current of the beam. A separate population of suprathermal electrons were also detected at these times. The pulse aftereffects persisted for approximately 15 ms before the plasma returned to its pre-pulse quiet state.

Following tether disconnect the dominant probe responses were due to the hot plasma environment. Enhanced electron temperatures associated with the electron beam were detected by the mother payload out to 87 m from the active daughter corresponding to a perpendicular separation of 34 m. In addition, clearly defined aftereffects were also evident within a 61 m, or 24-m perpendicular, separation. Figure 7 is a plot of the current-dependent temperature enhancements measured by the ETP soon after tether separation. The dominant heating effect of the 80 mA emission is clearly evident in the plot. Similar responses were observed at larger distances although the magnitude of the responses were decreased.

The electric fields measured in the vicinity of the daughter payload produced systematic

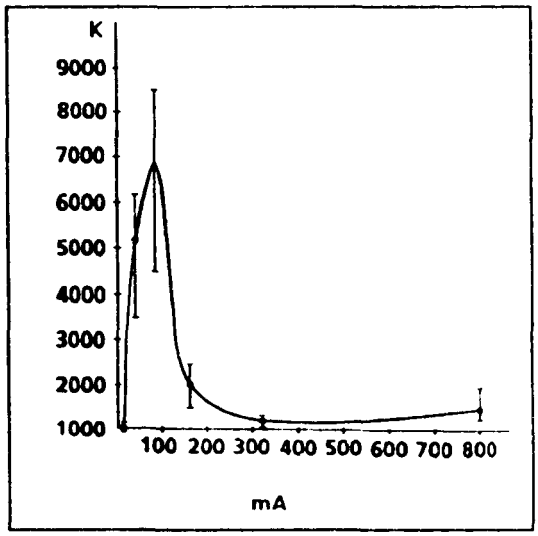

Figure 7. Electron temperature enhancements versus beam current during the pulse aftereffects.

responses to the pulsed beam which could be detected out to radial distances exceeding 60 m. Figure 8 is a representative sample of the electric field responses measured for different mother-daughter separation distances at a fixed current level of 160 mA. The data has been plotted in an instrument-centered coordinate system with no corrections for vehicle motion or contact potential variations. The legend accompanying each beam pulse specifies the time of flight (TOF), the pulse number, the injection pitch angle, the mother-daughter cross-field separation, and the altitude. The pulse signature within a radial distance of about 30 m was a onset impulse field of 1-to-2 ms followed by a persistent field lasting for at least the remainder of the pulse. In general the persistent electric fields could be measured at all beam current above 20 mA within the region of enhanced electron temperatures as measured with the ETP. Also, these persistent electric fields often could be measured for several milliseconds following beam termination. The impulse fields, on the other hand, were consistently measured only for currents greater than 80 mA but were detected well

outside the hot plasma region. The amplitude of the impulse field decreased with increasing radial distance and could not be detected beyond 65 m. For the remainder of this section, we restrict our attention to the impulse response features found during beam injections of 160 mA. In addition, for simplicity we will consider here only the perpendicular components of the electric field and ignore the complications introduced by the parallel component.

In order to present a synoptic view of the perpendicular electric field data from the MAIMIK experiment, a field-aligned coordinate system has been adopted which places the active daughter at the origin and fixes the azimuthal injection angle of the beam. Figure 9 is a plot of the 160-mA pulse data presented in this fixed coordinate system. Note the location of the daughter at the origin and the nominal trajectory of the 8-keV beam electrons injected along the positive Y axis. Beam electrons spiral in a clockwise direction with a nominal gyroradius of 6.2 m due to the downward pointing geomagnetic field. Changes in the gyroradius of the beam due to variations in the injection pitch angles and slight changes in the magnetic field strength during the course of the flight have been neglected in the plot. Also, the effects that a changing coordinate system might have on the morphology of the strong sheath can be neglected due to the small amplitude of the background field. Due to the increasing mother-daughter separation length and the spinning of the active payload between successive gun pulses the locus of points representing the mother's position during the successive 160-mA beam injections traces out a spiral in this coordinate system. The perpendicular projection of the corrected electric fields were then rotated into this normalized coordinate system and plotted at the determined locations of the mother. The advantage of this coordinate system is the clarity that it permits for representing the full set of field data on a single plot where the disturbance source is fixed at the origin.

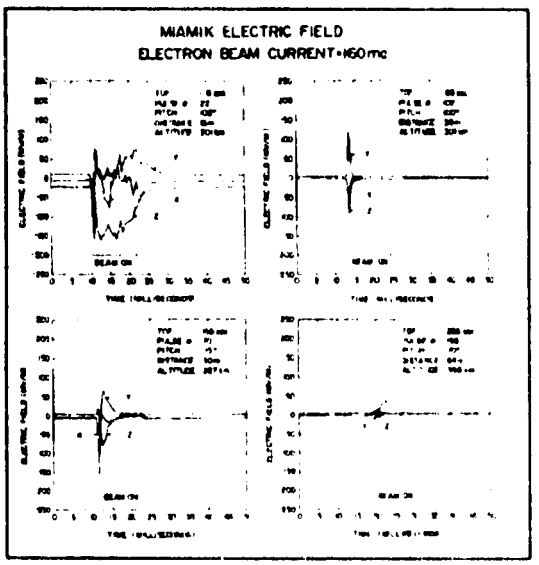

Figure 8. Uncorrected electric field responses versus separation distance for 160-mA beam pulses.

The 160-mA response data in Figure 9 indicate that the impulse fields had outward-pointing radial components and tangential, or azimuthal, components. The MAIMIK results make it clear that the tangential components produced a systematic pattern of counterclockwise deflections from the radial direction. Similar patterns were obtained for the 320 mA and 800 mA beam cases. Although the wave nature for the radial components is not immediately obvious in the data, the consistent counterclockwise deflections in the tangential fields strongly suggests that the azimuthal component must have been of electromagnetic origin. The similar time responses for the radial and tangential components further suggests that they were either part of the same wave train or were responding to the same driving source.

DISCUSSION

The analysis of data from the MAIMIK rocket experiment has so far concentrated on the observations of high charging, particularly the overcharging, of the daughter payload, the current-dependent heating of the background plasma, and the impulsive electric fields driven by the pulsed electron beam. These separate topics are, of course, quite interrelated although it is the overcharging mechanism which we believe is responsible for the unanticipated plasma heating effect (Svenes et al., 1988) and the generation of the impulsive electric fields (Denig et al., 1989). In this section, we carefully consider the experimental

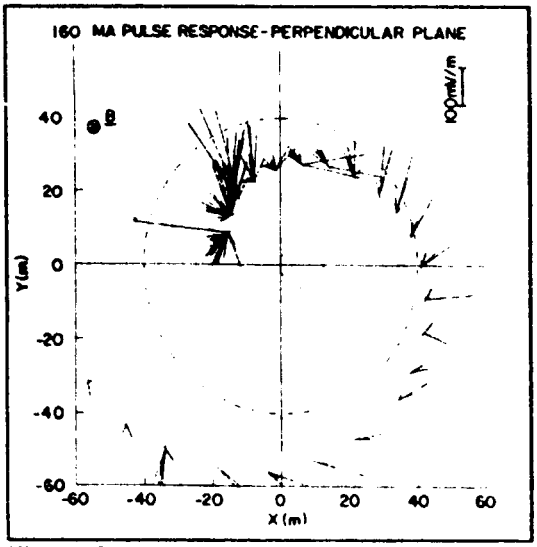

Figure 9. Summary plot of the corrected electric field signatures in a daughter centered coordinate system for 160-mA beam injections.

observations and formulate a physical description of the interaction among the active payload, the electron beam, and the background plasma.

The observation of extreme potential charging by the active daughter payload was not entirely anticipated prior to the MAIMIk flight. There had been an earlier indication that modest charging by a rocket-borne accelerator was possible (Jacobsen and Maynard, 1980) but the overcharging condition was a new and surprising result. MAIMIK was the first experiment to successfully test the tethered rocket concept during active electron emission although the technique had been demonstrated earlier for lower payload potentials (Williamson et al. (1982). Paramount in the use of a tether for potential measurements is the reliability of the ground reference. In the case of the MAIMIK experiment, there were several compelling reasons to suggest that the reference did not significantly deviate from the potential of the undisturbed background plasma. Specifically, the electric field measurements indicated that the vehicle was outside the region of intense potential gradients and that the integrated radial electric field beyond the mother was only a minor contributor to the daughter payload potential. Second, it was unlikely that the tether upset the ground reference since the 1.3 mA of current which flowed through the 10 Megohm tether during the largest potentials was easily drawn from the surrounding ionospheric plasma by the large surface area of the mother payload. Most conclusive, however, was the rather strong agreement between the tether voltage measurements and the energy distribution of the returning electron flux within the instrument capabilities of the RPA. For these reasons we believe that the high charging observations from the MAIMIK experiment were real.

A detailed examination of the active daughter payload was possible only for the initial gun operations occurring prior to tether disconnect at 113 s. However, the limited data set provided measurements over the full range of beam currents and was used to identify a current threshold in the overcharging mechanism. The experimental observations indicate that for the MAIMIK experiment this threshold occurred somewhere between 40 mA and 80 mA. We believe that this threshold represents the formation of a virtual cathode; that is, a turbulent region of negative space charge, near the electron gun aperture (Denig et al., 1987; Maehlum et al., 1988).

A virtual cathode is a naturally occurring phenomenon in the (near) vacuum propagation of intense electron beams when the injected current exceeds the space-charge limit defined by the system geometry (Miller, 1982). The existence of a virtual cathode has been suggested from laboratory space simulation experiments (Kellogg et al., 1982) and in space (Managadze et al., 1988).

The experimental conditions responsible for the formation of the virtual cathode during the MAIMIK rocket flight were the high beam-to-plasma density ratio and the small physical size of the daughter (Maehlum et al., 1988). The limited return current available from the ionosphere caused the initial high charging of the beam payload. Once the space-charge limit for the system was exceeded the virtual cathode formed and reflected the bulk of the beam back to the payload. The turbulent behavior of the cathode stocastically accelerated, via wave particle interactions, a portion of the primary electrons allowing a small percentage of the beam to escape the system and to thereby drive the payload into the

overcharged state.

The RPA data indicated that the daughter payload continued to charge to high potentials during beam operations until the rocket entered the mesosphere near the end of the flight (J. Triom, private communication, 1987). In most cases the vehicle potential exceeded the 3.2 kV maximum energy of the RPA but the instrument quickly recovered at the termination of the beam. During the post-pulse interval the instrument measured a suprathermal population of electrons near the gun-emitting payload which persisted for 10-to-20 ms. A suprathermal electron population was also measured by the ETP within a heated plasma region around the daughter.

The ETP measurements show that maximum electron heating occurred for the 80 mA beams and that the radial size of the disturbed plasma region was limited to within 34 m from the central body. The heated plasma near beam emitting payloads has been extensively studied using sounding rockets and supporting data from laboratory experiments (Grandal, 1982). The measured electron energy distribution within the interaction region of beam-plasma experiments shows the increased heating effect and the suprathermal acceleration of the background plasma by the beam (Jost et al., 1980). The sources of free energy available to create the suprathermal electrons and to heat the background electrons are the collisional effects of the beam and instability processes such as the two-stream instability (Arnoldy et al., 1985; Winckler and Erickson, 1986). The radial size of the heated region in space has been found to scale with the gyroradius of the primary beam and with the magnitude of the injected current (Duprat et al., 1983). The radial dimension of the heated plasma region on MAIMIK was about 6 gyro radii wide which scales well to some previous rocket results (Winckler and Erickson, 1986).

The observed current threshold in the electron heating efficiency by the MAIMIK electron beam was the direct result of the overcharging condition. Since the major portion of the electron beam was immediately reflected by the virtual cathode its effective reaction length with the local plasma was reduced and the local plasma heated to a lesser degree.

The measured recovery time of the background plasma following the termination of the beam pulse was much quicker than expected from collisional cooling effects and recombination. This suggests that the plasma thermalization occurred via some wave-particle interaction (Okuda and Abhour-Abdulla, 1988). This also implies that the beam-plasma interaction did not lead to significant background ionization during the pulse. It may be that the critical parameters for the onset of the Beam-Plasma Discharge (Bernstein et al., 1979) were not achieved during the MAIMIK flight.

The persistent electric fields measured within 30 m of the central body corresponded to the region of enhanced electron temperatures and were perhaps the residual effects of the outer sheath of the highly charged daughter payload. Although the persistent fields existed for all currents above 20 mA they were generally small and not very amenable to detailed analyses. The beam signatures of greater interest were the impulsive fields measured at the initiation of the beam pulses for currents above the overcharging threshold. Similar impulse fields were observed during the active POLAR 5 (Jacobsen and Maynard, 1980) and ECHO 6 (K. Ericksen, private communication, 1989) rocket experiments during periods when the payloads are believed to have charged to some high potential. However, the details of the impulse fields and the vehicle charging for these other rocket experiments were not fully addressed due to instrument limitations.

The MAIMIK impulse fields were consistent with the expected effects of ion dynamics driven by the sudden increase in the potential of the daughter at the beam initiation. A calculation of the equivalent vacuum capacitance for the daughter; that is, about 33 pF for the 30-cm sphere, shows that the excess charge needed for the daughter to reach 14 kV was accumulated within several microseconds of beam turn-on. On the other hand, the time scale for the formation of the high potential sheath was on the order of several ion plasma periods (Borovsky, 1988) or a fraction of a millisecond during which time the ions were expelled from the inner sheath region near the daughter. The ion blast wave was a

local source of spacecharge which generated the radial impulse fields. The momentary radial field then caused the local electrons to **ExB** drift well before the background ions could respond. The transient Hall current generated by the flowing charge in turn generated a time varying magnetic field which coupled into the azimuthal field via Faraday's Law. The magnitude and orientation of the calculated azimuthal field are consistent with the MAIMIK impulse electric field measurements (Denig et al., 1989).

CONCLUSIONS

The scenario which we feel describes the set of MAIMIK data described here is the following. The overcharging of the daughter payload during active electron emission was due to the combined effects of the low ionospheric plasma density and the small size of the payload. The physical mechanism responsible for the overcharging was virtual cathode formation near the gun aperture which reflected the major portion of the beam. On the other hand, the highly turbulent nature of the cathode energized a small fraction of the beam which then escaped the system and thereby sustained the discharged. Due to the reduced beam propagation above the current threshold for virtual cathode formation the beam-plasma interaction was greatly reduced and a minimum heating effect observed. The rapid charging of the daughter payload at beam initiation accelerated the local ions outward which, in turn, created a radial E-field at distant locations. This momentary field caused the background electrons to E x B drift azimuthally during an interval when the ions were fixed by their larger inertia. The time response of the induced current coupled into an azimuthal E-field via Faraday's Law.

ACKNOWLEDGEMENTS

WFD's efforts at GL in the preparation of this manuscript were supported by program element 62101F, project 7601, and by AFOSR under program element 61102F, task 2311G5. The MAIMIK rocket experiment was jointly sponsored by NASA (USA) and NTNF (NORWAY). The authors note the contributions of the following individuals in the MAIMIK analysis efforts; Drs. J. Triom, N.C. Maynard, W.J. Burke, M. Friedrich, K.M. Torkar, G.K. Holmgren, A.A. Egeland, T. Hansen, K. Maseide. B.T. Narheim, and J.D. Winningham.

REFERENCES

Arnoldy, R.L., C. Pollock, and J.R. Winckler, The energization of electron beams injected in the ionosphere, J. Geophys. Res., 90, 5197-5210, 1985.

Balmain, K.G. Impedance of a radio-frequency plasma probe with an absorptive surface, Radio Science, 1, 1-12, 1966.

Bernstein, W., H. Leinbach, P.J. Kellogg, S.J. Monson, T. Hallinan, Further laboratory measurements of the beam-plasma discharge, J. Geophys. Res., 84, 7271-7278, 1979.

Borovski, J.E., The dynamic sheath: Objects coupling to plasmas on electron-plasma-frequency time scales, Physics Fluids, 31, 1074-1100, 1988.

Cambou, F., V.S. Dokoukine, V.N. Ivchenko, G.G. Managadze, V.V. Migulin, O.K. Nazarenko, A.T. Nesmyanovich, A. Kh. Pyatsi, R.Z. Sagdeev, and I.A. Zhulin, The Zarnitza rocket experiment on electron injection, Space Research, XV, 491-500, 1975

Cartwright, D.G., S.J. Monson, and P.J. Kellogg, Heating of the ambient ionosphere by an artifically injected electron beam, J. Geophys. Res., 83, 16-24, 1978.

Coffey, H.E., Geomagnetic and solar data, J. Geophys. Res., 91, 3328, 1986.

Denig, W.F., N.C. Maynard, W.J. Burke, and N.C. Maynard, E-field measurements during electron beam emissions on MAIMIK, EOS, Trans. AGU, 68, 1400, 1987.

Denig, W.F., N.C. Maynard, W.J. Burke, and B.N. Machlum, Electric field measurements during supercharging events on the MAIMIK Rocket Experiment, submitted to J. Geophys. Res., 1989.

Duprat, G.R., B.A. Whalen, A.G. McNamara, and W. Bernstein, Measurements of the stability of energetic electron beams in the ionosphere, J. Geophys. Res., 88, 3095-3108, 1983.

Grandal, B., Artificial Particle Beams in Space Plasma Studies, 704 pp., Plenum, New York, 1982.

Hardy, D.A., M.S. Gussenhoven, and E.

Holeman, A statistical model of auroral electron precipitation, J. Geophys. Res., 90, 4229-4248, 1985.

Hess, W.N., M.C. Trichel, T.N. Davis, W.C. Beggs, G.E. Kraft, E. Stassinopoulos, and E.J.R. Maier, Artificial auroral experiment: experiment and principal results, J. Geophys. Res., 76, 6067-6081, 1971.

Jacobsen, T. A. and N. C. Maynard, POLAR 5 - An electron accelerator experiment within an aurora. 3. Evidence for significant spacecraft charging by an electron accelerator at ionospheric altitudes, Planet. Space Sci., 28, 291-307, 1980.

Jost, R.J., H.R. Anderson, and J.O. McGarity, Electron energy distributions measured during electron beam/plasma interactions, Geophys. Res. Letts., 7, 509-512, 1980.

Kellogg, P.J., H.R. Anderson, W. Bernstein, T.J. Hallinan, R.W. Holzworth, R.J. Jost, H. Leinbach, and E.P. Szuszczewicz, Laboratory simulation of injection particle beams in the ionosphere, in Artificial Particle Beams in Space Plasma Studies, edited by B. Grandal, pp. 289-329, Plenum, New York, 1982.

Maehlum, B.N., K. Maseide, K. Aarsnes, A. Egeland, B. Grandal, J. Holtet, T.A. Jacobsen, N.C. Maynard, F. Soraas, J. Stadsnes, E.V. Thrane, and J. Troim, POLAR 5 - An electron accelerator experiment within an aurora. 1. Instrumentation and geophysical conditions, Planet. Space Sci., 28, 259-278, 1980.

Maehlum, B.N., W.F. Denig, A.A. Egeland, M. Friedrich, T. Hansen, G. K. Holmgren, K. Maseide, N.C. Marnard, B.T. Narheim, K. Svenes, K. Torkar, J. Troim, and J.D. Winningham, MAIMIK - A high current electron beam experiment on a sounding rocket from Andoya Rocket Range, In Proc. 8th ESA Symposium on Rockets and Balloons, ESA SP-270, 261-265, 1987.

Maehlum, B.N., J. Troim, N.C. Maynard, W.F. Denig, M. Friedrich, and K.M. Torkar, Studies of the electrical charging of the tethered electron accelerator mother-daughter rocket MAIMIK, Geophys. Res. Lett., 15, 725-728, 1988.

Maehlum, B N., M. Friedrich, W.F. Denig, G. Holmgren, N.C. Maynard, W.J. Burke, K. Svenes, K.M. Torkar, and J. Troim, MAIMIK -A tethered "mother-daughter" electron accelerator rocket, Space Research, in press, 1989

Managadze, G.G., V.M. Balebanov, A.A. Burchudladze, T.I. Gagua, N.A. Leonov, S.B. Lyakov, A.A. Martinson, A.D. Mayorov, W.K. Reidler, M.F. Friedrich, K.M. Torkar, A.N. Laliashvili, Z. Klos, and Z. Zbyszynski, Potential observations of an electron-emitting rocket payload and other related plasma measurements, Planet. Space Sci., 36, 399-410, 1988.

Maynard, N. C., D. S. Evans and J. Troim, Electric field observations of time constants related to charging and charge neutralization processes in the ionosphere, in Artificial Particle Beams in Space Plasma Studies, edited by B. Grandal, pp. 627-644, Plenum, New York, 1982.

Miller, R.B., An Introduction to the Physics of Intense Charged Particle Beams, 351 pp., Plenum, New York, 1982.

Okuda, H. and M. Ashour-Abdulla, Ion acoustic instabilities excited by injection of an electon beam in space, J. Geophys. Res., 93, 2011-2015, 1988

Sagalyn, R.C., M. Smiddy, and J. Wisnia, Measurement and interpretation of ion density distributions in the daytime F region, J. Geophys. Res., 68, 199-211, 1963.

Svenes, K., J. Triom, M. Friedrich, K.M. Torkar, and G. Holmgren, Ionospheric plasma measurements from the accelerator rocket MAIMIK, Planet. Space Sci., 36, 1509-1522, 1988.

Williamson, P.R., W.F. Denig, P.M. Banks, W.J. Raitt, N. Kawashima, K. Hirao, K.I. Oyama, and S. Sasaki, Measurements of vehicle potential using a mother-daughter tethered rocket, in Artificial Particle Beams in Space Plasma Studies, edited by B. Grandal, pp. 645-653, Plenum, New York, 1982.

Winckler, J.R., The application of artificial electron beams in magnetospheric research, Rev. Geophys. Space Phys., 18, 659-682, 1980.

Winckler, J.R. and K.N. Erickson, Plasma heating, plasma flow and wave production around an electron beam injected into the ionosphere, in Space Technology Plasma Issues in 2001, ed. H. Garrett, J. Feynman, and S. Gabriel, JPL Publication 86-49, pp. 295-306, 1986